https://doi.org/10.62836/jcmea.v3i1.030109

Global Science Publishing

JCMEA

Journal of Computational Methods in Engineering Applications

https://ojs.sgsci.org/journals/jcmea

Article

Enhanced E-Commerce Sales Forecasting Using EEMD-Integrated LSTM Deep Learning Model

Yunxiang Gan [1], Jiahuai Ma [2] and Kaixian Xu [3,*]

[1] *Moloco, CA, USA; yg281@scarletmail.rutgers.edu*

[2] *Gainesville, Fl, USA; maj2@ufl.edu*

[3] *Jersey City, NJ, USA*

Abstract: E-commerce sales data often exhibit complex time series characteristics and are influenced by multiple factors, making traditional forecasting methods inadequate in capturing these dynamics. To address these challenges, this paper presents a forecasting model that integrates Ensemble Empirical Mode Decomposition (EEMD) with Long Short-Term Memory (LSTM) networks. The model first applies EEMD to decompose the original data signal into multiple Intrinsic Mode Function (IMF) components. These components, along with the original data, are then fed into the LSTM network for predictive analysis. As a case study, the proposed model is tested using a sales dataset of an Amazon clothing product. The results demonstrate that the model achieves a forecasting accuracy of 91%, surpassing several commonly used forecasting approaches in precision and reliability. This study highlights the potential of the EEMD-LSTM approach in improving sales forecasts for e-commerce platforms.

Keywords: forecasting model; e-commerce sales data; ensemble empirical mode decomposition; deep learning

1. Introduction

The rapid advancement of internet technologies has propelled e-commerce into a pivotal role in global business, reshaping consumer behavior and transforming market structures. The vast amount of sales data generated by e-commerce platforms captures not only detailed consumer behavior but also offers insights into market trends, consumer preferences, and emerging business opportunities [1, 2]. In China, with the transformation of the overseas study consulting industry and the gradual application of data analytics, more and more industries are exploring how to extract key information from big data to support future decision-making [3]. Leveraging this data through accurate forecasting can empower businesses to make informed decisions, mitigate risks, and seize new opportunities.

Sales forecasting is a critical chapter in e-commerce, enabling companies to predict future trends based on historical data. It supports effective production planning, inventory management, and strategic marketing adjustments, ultimately enhancing competitiveness in dynamic markets [4,5]. Accurate forecasts help businesses align supply with demand, reduce operational costs, and optimize marketing efforts to capture seasonal or promotional opportunities. In addition, research on green supply chain optimization in global supply chain management and the chemical industry provides a broader perspective for supply chain management in e-

Received: 19 October 2023; Accepted: 6 November 2023.

* Corresponding: Kaixian Xu (kx374@nyu.edu)

commerce [6,7].

Among the various forecasting methods, time series analysis is particularly suitable for e-commerce due to its ability to detect temporal patterns and capture fluctuations over time. This approach allows businesses to anticipate sales trends and account for seasonal variations, promotional events, and shifting consumer demand [8]. However, precise forecasting of e-commerce sales data remains challenging due to its inherent complexity, influenced by dynamic, nonlinear factors and multi-dimensional variability [9]. Research on luxury brand reputation reveals that data decomposition techniques can precisely capture subtle shifts in consumer patterns within multidimensional markets [10,11].

To address these challenges, signal decomposition techniques are often applied to enhance the interpretability and accuracy of time series models. Empirical Mode Decomposition (EMD), for example, has been widely studied for its ability to extract meaningful components from complex data. Researchers such as P. E. S. and M. A. N. V. introduced a wavelet-based denoising method for EMD to enhance the quality of signal decomposition [12]. Although this approach showed improved denoising performance, it faced issues like mode mixing and algorithm instability. Similarly, Parey A. et al. explored EMD for fault diagnostics, effectively decomposing vibration signals, but encountered the endpoint effect, hindering reliable signal reconstruction [13]. Moreover, the application of Generative Adversarial Networks (GANs) in image recognition and user behavior prediction has demonstrated the potential of signal decomposition and denoising techniques in handling complex e-commerce data [14,15].

Given these limitations, Ensemble Empirical Mode Decomposition (EEMD) was developed as an improvement over EMD. EEMD introduces noise-assisted decomposition to mitigate mode mixing, thereby enhancing the stability and reliability of forecasts.

The final step in time series forecasting models involves deep learning algorithms, which significantly impact the accuracy of classification and recognition. Traditional time series analysis methods, such as the ARIMA model and exponential smoothing method, can capture linear trends and seasonal variations to some extent; however, they are inadequate for handling complex dynamic nonlinear system data [16, 17]. This limitation is especially apparent when encountered with time series data like e-commerce sales and stock price. With the rise of artificial intelligence, intelligent algorithms such as Support Vector Machines (SVM), Extreme Learning Machines (ELM), Convolutional Neural Networks (CNN), and Long Short-Term Memory (LSTM) networks have been developed and widely applied in various complex time series forecasting problems [18]. Among these, Recurrent Neural Networks (RNN) and their variant-LSTM-are become popular in deep learning [19]. Because LSTM, as a specialized architecture of RNN, effectively addresses the gradient vanishing and explosion issues that traditional RNNs face when processing long sequences [20,21].

The LSTM algorithm has demonstrated significant potential in practical applications. In the e-commerce sector, Yongsu K. pioneered the use of LSTM to forecast product sales and analyze purchasing behavior, achieving a prediction accuracy of 90% [22]. Similarly, Ly T. S. utilized LSTM in the financial sector for stock price prediction and risk assessment, finding that its accuracy significantly outperformed common deep learning methods like CNN, with a prediction accuracy as high as 97% [23]. These studies highlight the effectiveness of LSTM for tackling complex, nonlinear time series data and underscore its relevance for sales forecasting in e-commerce. Recent advances in multifunctional OCR models for noise handling have expanded deep learning's potential in complex data applications [24].

Building on these advancements, this paper proposes a hybrid forecasting model that combines EEMD with LSTM deep learning to address the challenges of forecasting e-commerce sales data. By applying EEMD to extract key intrinsic components from noisy sales data and applying LSTM to monitor temporal dependencies, the proposed model achieves high prediction accuracy. Additionally, the model construction draws on adaptive interaction models for trajectory prediction to ensure flexibility and stability in e-commerce data applications, while also leveraging the linear layering structure of deep UV LEDs to optimize algorithm performance [25,26]. Using a clothing sales dataset from Amazon, available in the UCI Machine Learning Repository, this study validates the effectiveness of the model.

2. Theoretical Foundations

2.1. Empirical Mode Decomposition Method

The EMD algorithm is an adaptive signal processing technique that decomposes complex, mixed signals into multiple Intrinsic Mode Functions (IMFs). This decomposition allows for the separation of composite signals into distinct components, facilitating more accurate analysis. Unlike Fourier transforms and wavelet transforms, EMD adaptively decomposes signals based on their length and complexity, without requiring a predefined basis function. This adaptability ensures a high signal-to-noise ratio and provides effective time-frequency localization.

The EMD algorithm performs decomposition by extracting IMFs that represent oscillatory modes embedded within the original signal. The resulting IMFs capture both amplitude and frequency variations, making the method particularly useful for analyzing non-stationary and nonlinear signals. To ensure the decomposition is valid, the extracted IMF components must satisfy the following two conditions:

1. For the entire sample dataset, the difference between the number of zero-crossings and the number of extreme points (local maxima or minima) must be less than or equal to 1;

2. Throughout the decomposition process, the mean value of the upper envelope (connecting the local maxima) and the lower envelope (connecting the local minima) must always be 0.

The EMD method extracts the IMF vectors through a sifting process, which iteratively removes the local averages of the upper and lower envelopes. Each IMF is obtained through the following steps:

First, calculate the mean envelope $y_1(t)$ of the original signal.

$$y_1(t) = \frac{y_+(t) + y_-(t)}{2} \tag{1}$$

where $y_+(t)$ and $y_-(t)$ represent the upper and the lower envelope function fitted to the original signal, respectively.

To obtain the $h_1^1(t)$ that does not contain low-frequency signals, subtract $y_1(t)$ from the original signal $x(t)$ as shown in the Equation (2).

$$h_1^1(t) = x(t) - y_1(t) \tag{2}$$

Determine whether $h_1^1(t)$ meets the two conditions for IMF decomposition. If not, repeat these steps after k iterations until the two conditions are satisfied. Then, the first-order IMF component of the original signal is $c_1(t)$, and can be expressed as:

$$c_1(t) = imf_1(t) = h_1^k(t) \tag{3}$$

Generally, k is less than 10.

Abstract $c_1(t)$ from the original signal to generate a new signal $r_1(t)$, $r_1(t)$ is expressed by Equation (4):

$$r_1(t) = x_1(t) - c_1(t) \tag{4}$$

Repeat the above steps of Equations (1) and (2) for $r_1(t)$ until $r_1(t)$ meets the IMF conditions, resulting in the second IMF component $c_2(t)$. Continue this process until obtaining the n-th order IMF component $c_n(t)$, with the residue $r_n(t)$being a monotonic function. The decomposition process will stop when the IMF conditions can no longer be accomplished.

The decomposition result of EMD is:

$$x(t) = \sum_{i=1}^{n} c_i(t) + r_n(t) \tag{5}$$

where $r_n(t)$ is the final residual; n is the number of IMFs. Within the decomposition frequency range, EMD decomposition yields n IMF vectors corresponding to different frequencies, which are then sorted from high to low frequency.

The EMD decomposition algorithm is characterized by its fast solution speed and strong adaptability. However, it still faces challenges such as mode mixing and endpoint effects.

2.2. The Ensemble Empirical Mode Decomposition

Ensemble Empirical Mode Decomposition (EEMD) is an improved version of the Empirical Mode EMD technique. It works by adding white noise to the EMD algorithm, guiding the classification of signals and enabling the automatic separation of pure signals with different frequencies. EEMD effectively resolves the mode mixing issue inherent in the original EMD algorithm, greatly enhancing the accuracy of signal decomposition.

The computational steps of the EEMD algorithm are as follows:

First, Set the number of times white noise is added to N. Add one time of Gaussian white noise $\rho_1(t)$ to the original signal $x(t)$ to form the mixed signal $X_1(t)$.

$$X_1(t) = x(t) + \rho_1(t) \tag{6}$$

Decompose the mixed signal $X_1(t)$ using EMD. The decomposition yields multiple intrinsic mode functions (IMFs) with different frequencies:

$$X_1(t) = \sum_{i=1}^{m} IMF_{i,1}(t) + r_1(t) \tag{7}$$

where m is the number of IMFs obtained through EMD, and $r_1(t)$ is the residual component.

Add white Gaussian noise (WGN) signals across different frequency bands to the original signal, and repeat the first and second steps. The resulting $X_k(t)$ represents that $x(t)$ is decomposed by EEMD with K times:

$$X_k(t) = \sum_{i=1}^{m} IMF_{i,k}(t) + r_k(t) \tag{8}$$

To effectively eliminate the noise components in the signal, the average of all IMF components is computed.

$$IMF_i(t) = \frac{1}{N}\sum_{k=1}^{N} IMF_{i,k}(t) \tag{9}$$

Perform signal envelope reconstruction on the decomposed components $IMF_i(t)$, ensuring that the relationship between the reconstructed signal and the original signal is expressed as follows:

$$\omega_n = \frac{\omega}{\sqrt{N}} \tag{10}$$

where ω represents the standard deviation of the added white noise, while N denotes the times of noise added. It can be observed that ω_n decreases as the number of added noise increases. In this study, we ω = 0.2, and $N = 500$.

2.3. LSTM Network

The German scholars Hochreiter and Schmidhuber first introduced a recurrent neural network capable of remembering long-term dependencies, known as LSTM. LSTM is an enhanced deep learning method based on traditional recurrent neural networks, retaining their powerful memory capabilities while effectively capturing nonlinear features in time series data and accurately representing the temporal relationships among data points. The basic structure of a LSTM unit is illustrated in Figure 1 [27].

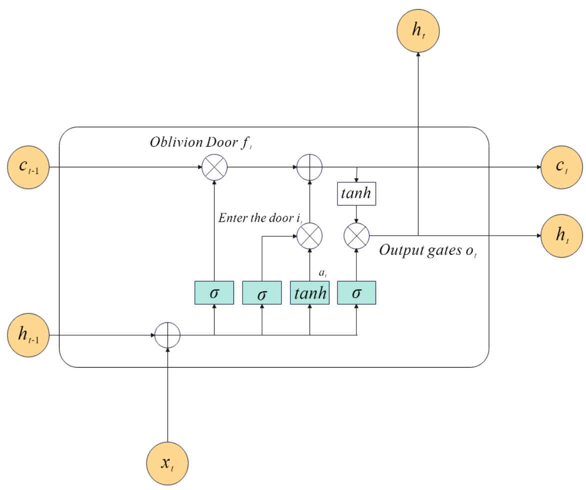

Figure 1. LSTM Basic Unit Diagram.

In the LSTM model, the Sigmoid activation function governs the forget gate, which primarily determines the noise information to be discarded from the previous long-term state $c_t - 1$. The expression for the f_t is presented in Equation (11). Through this mechanism, LSTM effectively manages the retention and forgetting of information.

$$f_t = \sigma\left(W_{xf}^T x_t + W_{hf}^T h_{t-1} + b_f\right) = \sigma\left(\overline{f_t}\right) \tag{11}$$

where f_t denotes the control of the forget gate, W_{xf}^T represents the dimensionality of the input features, W_{hf}^T signifies the dimension of the hidden layer features, $x_t$indicates the values of the input layer, h_{t-1} refers to the number of stacked LSTM layers, b_f represents the state values of the hidden layer, and $\sigma\left(\overline{f_t}\right)b$ denotes the values of the output layer.

In the LSTM model, the Sigmoid activation function plays a crucial role, primarily in controlling the input gate i_t. The expression for the Sigmoid function is presented in Equation (12), which enables the LSTM model to manage the flow and updating of information more precisely when processing time-series data.

$$i = \sigma\left(W_{xi}^T + W_{ht}^T h_{t-1} + b_i\right) = \sigma\left(\overline{i_t}\right) \tag{12}$$

In the LSTM model, the tanh activation function plays a crucial role in regulating the degree of integration between the current input and the long-term state c_t. Through the tanh function (see Equation (13)), the LSTM model effectively controls the interaction between the input information and the long-term state. This mechanism allows the LSTM to better capture and express the complex relationships among data when handling time-series information.

$$a_t = \tanh\left(W_{xa}^T x_t + W_{ha}^T h_{t-1} + b_a\right) = \tanh\left(\overline{a_t}\right) \tag{13}$$

The outputs of the forget gate f_t and the input gate i_t together influence the updating process of the long-term state c_t, as illustrated in Equation (14). This updating mechanism allows the LSTM model to integrate information from both forgetting and input, enabling it to capture and process complex patterns in time-series data more effectively.

$$c = f_t \otimes c_{t-1} + i_t \otimes a_t \tag{14}$$

where i_t is the input gate, and a_t is the hidden layer coefficient.

The output gate o_t uses the Sigmoid activation function to determine the short-term state h_t of the current neuron cell. The Sigmoid function is vital in this process, as it helps the LSTM model to decide which information will be output as the short-term state, thereby influencing the model's predictions and decisions. By employing the calculation method outlined in Equation (15), the LSTM can capture and utilize key features in time-series data more effectively.

$$o_t = \sigma\left(W_{xo}^T x_t + W_{ho}^T h_{t-1} + b_a\right) = \sigma\left(\overline{o_t}\right) \tag{15}$$

The determination of the short-term state involves integrating information from the current long-term state c_t and the output gate o_t. The calculation process is presented in Equation (16).

$$h_t = o_t \otimes \tanh\left(c_t\right) \tag{16}$$

When all control gates are removed and the long-term and short-term states are integrated, the LSTM unit effectively reverts to a standard recurrent neural network.

2.4. Prediction Model Based on EEMD and LSTM

Since traditional forecasting methods often struggle with complex, nonlinear, and fast-changing time series data. To overcome these challenges, this paper proposes a novel EEMD-LSTM model for the sales data prediction of a specific Amazon clothing product [28]. The process consists of several steps: First, the sales data undergoes preprocessing. Next, the EEMD method decomposes the data into multiple Intrinsic IMF components. Features are then extracted from these IMF components, forming a signal feature vector dataset, which is then fed into corresponding prediction models. Finally, the LSTM neural network algorithm fits the sales data, producing the final sales forecast results.

2.5. Evaluation Metrics

In evaluating the effectiveness of the prediction model, metrics include Root Mean Square Error (RMSE), Mean Absolute Error (MAE), Mean Absolute Percentage Error (MAPE), and the coefficient of determination (R^2) are generally used. However, due to the presence of zero values in the sales data of the specific Amazon clothing product, MAPE is not a suitable criterion for assessment. Therefore, this paper utilizes RMSE, MAE, and R^2 as the primary measurement standards, with the specific formulas outlined as follows.

$$RMSE = \sqrt{\frac{1}{n}\sum_{i=1}^{n}\left(y_i - x_i\right)^2} \tag{17}$$

$$MAE = \frac{1}{n}\sum_{i=1}^{n}\left|y_i - x_i\right| \tag{18}$$

$$R^2 = 1 - \sum_{i=1}^{n}\frac{\left(y_i - x_i\right)^2}{\left(y_i - \hat{y}\right)^2} \tag{19}$$

where x_i represents the actual value, y_j represents predicted value, and n denotes the number of data points.

The range for R^2 is between 0 and 1. A value of R^2 closer to 1 indicates a better fit of the model to the data. Generally, a model is considered as have a good fit when R^2 exceeds 0.8.

3. Empirical Analysis

3.1. Data Sources and Preprocessing

To thoroughly investigate the applicability of proposed method in forecasting clothing product sales on the Amazon e-commerce platform, this study utilizes a sample dataset of clothing sales obtained from the UCI Machine Learning Repository, covering the period from 1 October 2021, to 31 December 2021 (see Figure 2). As illustrated in Figure 2, the Amazon platform's clothing sales data exhibits complex and non-stationary characteristics, with observable periodic variations, indicating a close relationship between sales revenue and seasonal trends.

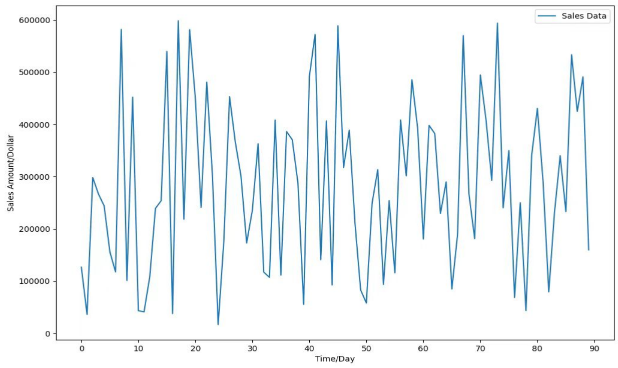

Figure 2. Amazon E-commerce Clothing Product Sales Sample Data.

Given the inherent instability of e-commerce sales data, the original dataset was normalized to enhance processing efficiency and accuracy, as displayed in Equation (20). The normalized data was then divided, with 90% allocated to the training set for model learning, and the remaining 10% used as the test set to evaluate the predictive accuracy of various algorithmic models. This partitioning ensures an objective performance assessment of the models in tackling the complex and dynamic challenges of e-commerce sales forecasting, providing robust data support for selecting the optimal prediction model.

$$x^1 = \frac{x - x_{\min}}{x_{\max} - x_{\min}} \tag{20}$$

where x^1 indicates the normalized data, $x_{\max}$ and $x_{\min}$ represent the maximum and minimum values in the sample, respectively.

In terms of neural network parameter settings, the model consists of two LSTM hidden layers, each with 32 neurons, along with a single-neuron output layer. The batch size is set to 16, and the model is trained for 200 epochs. An early stopping strategy was employed to prevent overfitting, and the Adam optimizer (Adaptive Moment Estimation) was selected and used. To ensure the stability of the results, the average of ten training outcomes for each model is taken as the final performance metric.

3.2. Signal Decomposition Processing

This study employed the EMD, EEMD, and CEEMD (Complete Ensemble Empirical Mode Decomposition) algorithms for signal decomposition on training sample data, with results illustrated in Figures 3 – 5. The decomposed IMF signal components exhibit a gradually flattening trend, indicating that interference signals are characterized by significant volatility. This observation suggests that multimodal decomposition methods can effectively eliminate these interference components from the data. High-frequency IMF components capture rapid oscillations in the signal, while low-frequency IMF components represent slower trends. The larger fluctuations observed in the low-frequency components indicate substantial changes in the signal, reflecting potential sudden events in e-commerce sales data. Consequently, this pronounced uncertainty and susceptibility to interference pose challenges for accurately forecasting e-commerce sales.

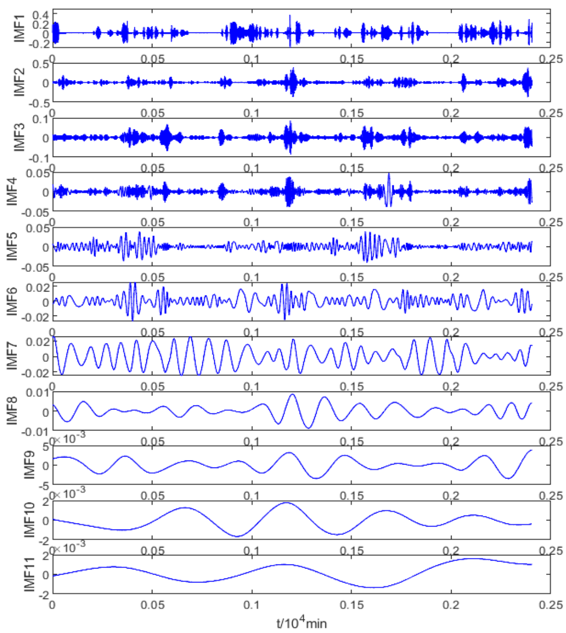

Figure 3. EMD Model Decomposition Results.

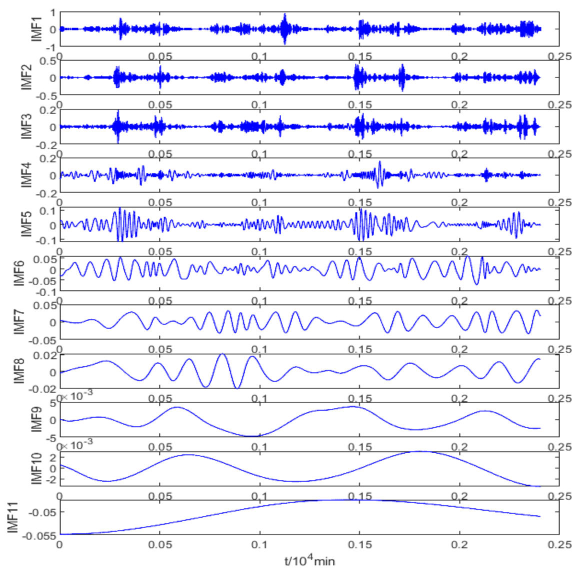

Figure 4. EEMD Model Decomposition Results.

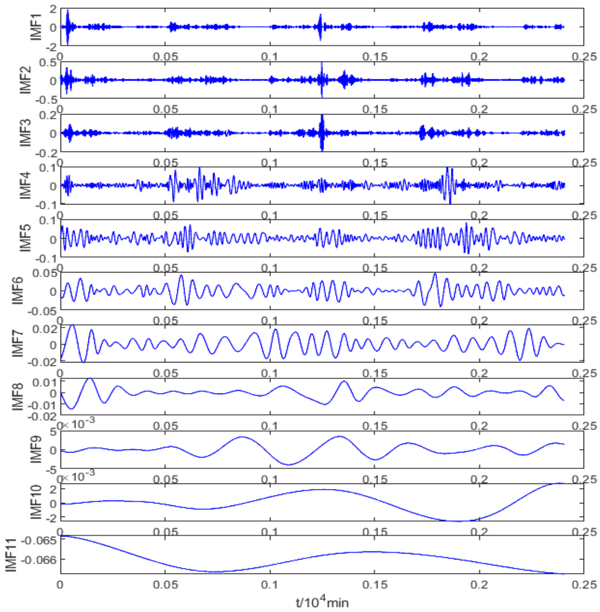

Figure 5. CEEMD Model Decomposition Results.

3.3. Analysis of the Results

To evaluate the effectiveness of different modal decomposition methods, this study inputs the IMF components from the EMD, EEMD, and CEEMD algorithms, along with the normalized training data, into both LSTM and back propagation (BP) models, creating six combined forecasting models: EMD-BP, EMD-LSTM, EEMD-BP, EEMD-LSTM, CEEMD-BP, and CEEMD-LSTM. A comprehensive comparison of these six models is then conducted, with the results presented in Table 1.

Table 1 is the corresponding results [29, 30]. Generally speaking, the EEMD-LSTM models achieve the highest R^2 values, while demonstrating the lowest RMSE and MAE values. This indicates that the proposed method performs better than other comparative models, highlighting its effectiveness in predicting e-commerce sales data.

Table 1. Comparative Analysis Table of Different Prediction Methods.

Prediction Method	R^2	RMSE	MAE
EMD-BP	0.8630	69.2230	61.4951
EMD-LSTM	0.9146	39 2848	31.2912
CEEMD-BP	0.9385	37.5875	29.0713
CEEMD-LSTM	0.9467	34.0916	27.3481
EEMD-BP	0.9638	29.1603	20.3052
EEMD-LSTM	0.9932	23.0854	15.2966

Specifically, the R^2 of the EEMD-LSTM combined model is the highest among the various methods, improving by nearly 3% compared to the EEMD-BP method, about 5% over the CEEMD-LSTM method, and approximately 6% over the CEEMD-BP method. This indicate that the proposed method provides the best fitness, effectively predict the sales for Amazon's e-commerce clothing products. Moreover, the EEMD-LSTM model achieves the lowest RMSE and MAE across all methods. Specifically, the corresponding RMSE and MAE of the EEMD-LSTM is approximately 20% and 25% lower than that of the EEMD-BP method, about 32% and 44% lower than that of the CEEMD-LSTM method, and around 38% and 47% lower than that of the CEEMD-BP method. These results further highlight the advantages of the proposed method in terms of prediction accuracy and affirm its robust identification capability.

In addition, the LSTM model outperforms the BP model in capturing the complex and highly nonlinear features of e-commerce sales data, demonstrating its superior prediction accuracy in the test. By employing the proposed method, a comparative analysis of the sales data from 1 December to 3 December 2021 were conducted (Figure 6). The results illustrate that the model fits the data exceptionally well, with only minor errors observed at certain extreme points, such as local maximum and minimum sales [31]. Overall, the predicted data closely aligns with the actual data, confirming the practical effectiveness of the constructed EEMD-LSTM model. By applying the LSTM neural network prediction model to analyze sales sample data for a specific e-commerce clothing product on Amazon from 1 December to 3 December 2021, we achieved a prediction accuracy of 91%.

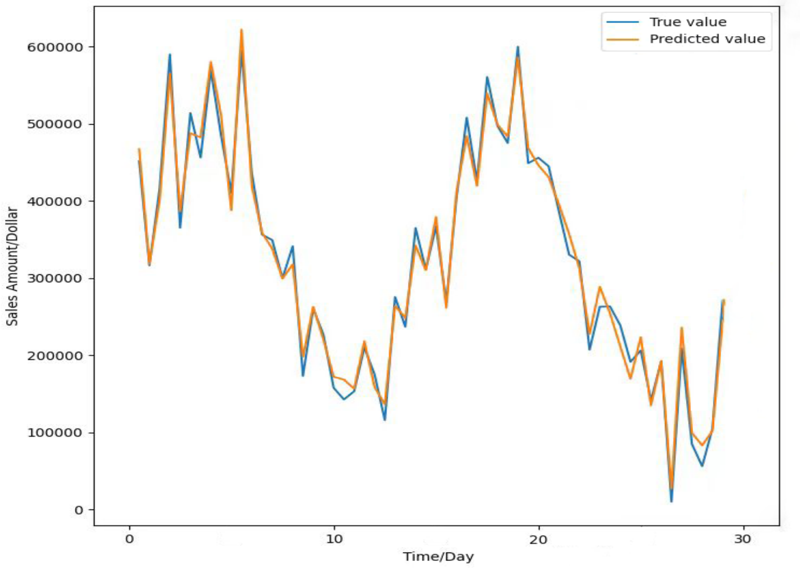

Figure 6. EEMD-LSTM Combined Model Prediction Results.

4. Conclusions

This paper combines the LSTM model with several advanced data decomposition algorithms to develop forecasting models, including EMD-LSTM, EEMD-LSTM, etc., for predicting Amazon clothing sales. The results demonstrate that the EEMD-LSTM model outperforms other methods:

1. Among the six forecasting methods analyzed, the EEMD-LSTM model achieved the highest R^2 score and the lowest RMSE and MAE values, confirming its superior predictive accuracy for the Amazon clothing sales dataset.

2. A test was conducted using sales data from 1 December to 3 December 2021. The EEMD-LSTM model maintained high accuracy, with predicted values closely matching the actual data. Its prediction accuracy reached 91%, further confirmed the model's reliability and effectiveness in practical applications.

Funding

Not applicable.

Author Contributions

Writing—original draft preparation, Y.G., J.M. and K.X.; writing—review and editing, Y.G., J.M. and K.X.; All of the authors read and agreed to the published the final manuscript.

Institutional Review Board Statement

Not applicable.

Informed Consent Statement

Not applicable.

Data Availability Statement

Not applicable.

Conflicts of Interest

The authors declare no conflict of interest.

References

1 Xin X, Jia N, Ling S, He Z. Prediction of Pedestrians Wait-or-Go Decision Using Trajectory Data Based on Gradient Boosting Decision Tree. *Transportmetrica B: Transport Dynamics* 2022; **10**(**1**): 693–717.

2 Kesavan S, Gaur V, Raman A. Do Inventory and Gross Margin Data Improve Sales Forecasts for U. S. Public Retailers?. *Management Science* 2010; **56**(**9**): 1519–1533.

3 Ren P, Zhao Z, Yang Q. Exploring the Path of Transformation and Development for Study Abroad Consultancy Firms in China. *arXiv* 2024; arXiv:2404.11034.

4 Seto H, Oyama A, Kitora S, Toki H, Yamamoto R, Kotoku JI, Moriyama T. Gradient Boosting Decision Tree Becomes More Reliable than Logistic Regression in Predicting Probability for Diabetes with Big Data. *Scientific Reports* 2022; **12**(**1**): 833–847.

5 Farnocchia MW, Robert High-Fidelity Comet67P Ephemeris and Predictions Based on Rosetta Data. *Icarus: International Journal of Solar System Studies* 2021; **358**(**1**): 114276.

6 Lei J. Green Supply Chain Management Optimization Based on Chemical Industrial Clusters. *arXiv* 2024; arXiv:2406.00478.

7 Lei J, Nisar A. Investigating the Influence of Green Technology Innovations on Energy Consumption and Corporate Value: Empirical Evidence from Chemical Industries of China. *Innovations in Applied Engineering and Technology* 2023; **2**(**1**): 1–16.

8 Rather AM. Deep Learning and Autoregressive Approach for Prediction of Time Series Data. *Journal of Autonomous Intelligen* 2020; **3**(**2**): 1–10.

9 Zhao Z, Ren P, Tang M. Analyzing the Impact of Anti-Globalization on the Evolution of Higher Education Internationalization in China. *Journal of Linguistics and Education Research* 2022; **5**: 15–31.

10 Li C, Tang Y. The Factors of Brand Reputation in Chinese Luxury Fashion Brands. *Journal of Integrated Social Sciences and Humanities* 2023; 1–14.

11 Zhu D, Gan Y, Chen X. Domain Adaptation-Based Machine Learning Framework for Customer Churn Prediction Across Varing Distributions. *Journal of Computational Methods in Engineering Applications* 2021; **1**(**1**): 1–14.

12 Scheijbeler EP, van Nifterick AM, Stam CJ, Hillebrand A, Gouw AA, de Haan W. Network-Level Permutation Entropy of Resting-State MEG Recordings: A Novel Biomarker for Early-Stage Alzheimer's Disease?*Network Neuroscience* 2022; **6**(**2**): 382–400.

13 Parey A, Badaoui ME, Guillet F, Tandon N. Dynamic Modelling of Spur Gear Pair and Application of Empirical Mode Decomposition-Based Statistical Analysis for Early Detection of Localized Tooth Defect. *Journal of Sound and Vibration* 2006; **294**(**3**): 547–561.

14 Xiong S, Zhang H, Wang M. Ensemble Model of Attention Mechanism-Based DCGAN and Autoencoder for Noised OCR Classification. *Journal of Electronic & Information Systems* 2022; **4**(**1**): 33–41.

15 Xiong S, Zhang H, Wang M, Zhou N. Distributed Data Parallel Acceleration-Based Generative Adversarial Network for Fingerprint Generation. *Innovations in Applied Engineering and Technology* 2022; **1**(**1**): 1–12.

16 Ma C, Tan L, Xu X. Short-Term Traffic Flow Prediction Based on Genetic Artificial Neural Network and Exponential Smoothing. *Faculty of Transport Traffic Sciences* 2020; **6**: 747–760.

17 Yahaya A, Etuk E, Emeka A. Comparative Performance of Arima and Garch Model in Forecasting Crude

Oil Price Data. *Asian Journal of Probability and Statistics* 2021; **15**(**4**): 251–75.

18 Berrich Y, Guennoun Z. Handwritten Digit Recognition System Based on CNN and SVM. In Proceedings of the 2022 CS & IT Conference Proceedings, Dubai, UAE, 17–18 December 2022.

19 Metlapalli AC, Muthusamy T, Battula BP. Classification of Social Media Text Spam Using VAE-CNN and LSTM Model. *Ingénierie des Systèmes D Information* 2020; **25**(**6**): 747–53.

20 Wang H, Li F. A Text Classification Method Based on LSTM and Graph Attention Network. *Connection Science* 2022; **34**(**1**): 2466–2480.

21 Ghosh I, Dragan P. Can Financial Stress Be Anticipated and Explained? *Uncovering the Hidden Pattern Using EEMD-LSTM*, EEMD-Prophet, and XAI Methodologies. *Complex Intelligent System* 2023; **9**(**4**): 4169 –4193.

22 Kim Y, Lee S, Kim H. Prediction Method of Photovoltaic Power Generation Based on LSTM Using Weather Information. *The Journal of Korean Institute of Communications and Information Sciences* 2019; **44**(**12**): 2231–2238.

23 Ly ST, Lee GS, Kim SH, Yang HJ. Gesture-Based Emotion Recognition by 3D-CNN and LSTM with Keyframes Selection. *International Journal of Contents* 2019; **15**(**4**): 59–64.

24 Xiong S, Chen X, Zhang H. Deep Learning-Based Multifunctional End-to-End Model for Optical Character Classification and Denoising. *Journal of Computational Methods in Engineering Applications* 2023; **2**(**1**): 1 –13.

25 Zhou Z, Wu J, Cao Z, She Z, Ma J, Zu X. On-Demand Trajectory Prediction Based on Adaptive Interaction Car Following Model with Decreasing Tolerance. In Proceedings of the 2021 International Conference on Computers and Automation (CompAuto), Virtual, 7–9 September 2021.

26 Chen X, Zhang H. Performance Enhancement of AlGaN-based Deep Ultraviolet Light-Emitting Diodes with AlxGa1-xN Linear Descending Layers. *Innovations in Applied Engineering and Technology* 2023; **2**(**1**): 1–10.

27 Guo Z, Liu M, Wang Y, Qin H. A New Fault Diagnosis Classifier for Rolling Bearing United Multi-Scale Permutation Entropy Optimize VMD and Cuckoo Search SVM. *IEEE Access* 2020; **8**: 153610–153629.

28 Mellahi K, Johnson M. Does It Pay to Be a First Mover in E. *Commerce? The Case of Amazon. com. Management Decision* 2000; **38**(**7**): 445–452.

29 Wang J, Li M, Dziatkovskii A, Hryneuski U, Krylova A. Research on Contour Feature Extraction Method of Multiple Sports Images Based on Nonlinear Mechanics. *Nonlinear Engineering* 2022; **11**: 347–354.

30 Yu M, Cong H, Chen W. A Research on Rubbing Feature Extraction Based on Information Fusion and Signal Decomposition Algorithm. *Noise Vibration Worldwide* 2022; **53**(**4-5**): 172–188.

31 Ma XY, Tong J, Jiang F, Xu M, Sun LM, Chen QY. Application of Deep Learning to Production Forecasting in Intelligent Agricultural Product Supply Chain. *Computers Materials Continua* 2023; **74**(**3**): 6145–6159.